Learning Based Estimation of 7 DOF Instrument and Grasping Forces on the da Vinci Research Kit

Jintan Zhang¹, Nural Yilmaz², Ugur Tumerdem², Peter Kazanzides¹

Abstract—Present-day minimally-invasive surgical robots, such as the da Vinci®, cannot directly sense interaction between the robotic instruments and the patient anatomy. This includes the instrument grasping force and the 6 degree-of-freedom (DOF) force/torque (wrench) between the instrument and the environment. Previous works have investigated model-based or data-driven methods that use available measurements, such as joint positions, velocities and torques, to estimate either the grasping force or the 6 DOF wrench. This paper extends prior work by developing and evaluating a data-driven (learningbased) method to simultaneously estimate the grasping force and external wrench. This task is complicated by the mechanical coupling between the gripper and other wrist joints, but the network is able to simultaneously estimate external forces, torques, and gripper force with RMS errors of 1.4 N, 0.04 Nm, and 0.1 N, respectively. In addition, transfer learning is shown to enable the neural network to quickly adapt to different instruments.

I. INTRODUCTION

Robotically assisted minimally invasive surgery systems (RAMIS) make use of teleoperated patient side robotic endoscopes and instruments boasting similar articulation capability to the human wrist and the ability to pass through small incisions to operate intracorporeally. They provide the benefits of conventional laparoscopic surgery to patients, such as reduced side effects, blood loss, scarring and recovery times. For the surgeons they provide increased ergonomy, better control over the surgical instrument through immersive 3D visual displays, direct mapping between hand motions and the instruments to eliminate the mirrored motion problem, wrist articulation, increased precision by motion scaling and tremor filtering. However, an important feature missing in the state of the art is that the interaction forces between the robotic instrument and the patient body cannot be felt by the surgeon operators while they are commanding the robots via the master interfaces. While in conventional laparoscopy the forces are transmitted to the surgeon's hand directly through the instruments, this is not possible with commercially available RAMIS systems due to several technical problems. One of the major obstacles is the difficulty in developing miniaturized force sensors that can be placed on the instrument tips, and although some research groups have successfully built force sensors [1]–[7] that can be placed on the instruments, it is difficult to maintain such systems in practice as the instruments are frequently changed during operations, need

to be sterilized and have extremely limited useful lives. This would make sensorization a costly endeavour.

An alternative approach to solve the force sensing issue is sensorless force estimation which can be achieved through proprioceptive robot measurements such joint positions obtained from encoders. Force estimation techniques have to account for the dynamics of the patient side manipulators, which can be difficult to identify due to the cable/pulley transmissions utilized for articulated wrist motions. For instance, commercially available robotic surgery systems like the da Vinci make use of Endowrist instruments which have designs that couple some of the roll-pitch-yaw-grasping motions with cable pulley transmissions. Furthermore, these transmissions suffer from nonlinear behavior such as slack and slip due to cable elasticity. Different mechanical designs have been proposed to overcome the coupling in the wrist and gripper joints in [8]–[11]. In [12]–[15], decoupling algorithms and methods have been proposed for specially developed surgical robots. However, these systems have yet to find widespread commercial applications in robotic surgery. The question then remains whether it is possible to account for dynamic coupling in wrist-gripper axes of commercially available robotic surgery systems.

Open source research platforms such as the da Vinci Research Kit [16], [17], and Raven II [18] can be used to develop methods to address this problem. In [19], the use of end-to-end learning is proposed by training machine learning algorithms with force sensor measurements to obtain accurate 3 DOF Cartesian force estimates on the dVRK. An alternative approach is to identify the dynamics of robot manipulators and to estimate the external force from joint torque measurements and the robot Jacobian by filtering out the dynamic torques. Model based approaches can be utilized for identification as suggested in [20], [21] for the dVRK and [22] for Raven II. These approaches have been used to obtain Cartesian 3 DOF [23] and 6 DOF [24] force estimation. While these methods can accommodate for the cable elasticity to some extent, they assume either that the coupling between the robot wrist and gripper is only due to dynamics, or that any non-dynamic coupling, such as due to the transmission, has been corrected. In the case of dVRK, it is well known that the joint-actuator coupling matrix provides the kinematic description of the coupling in the joints, however it is not clear whether the coupling matrix is adequately compensating for this effect. In [25], [26], end-to-end deep learning with ground truth force/torque sensors have been proposed to estimate 1 DOF grip forces and [25] addresses decoupling in the gripper axis of da Vinci Endowrist instruments implicitly

¹Dept. of Computer Science, Johns Hopkins University, Baltimore, MD 21218, USA (email: {jzhan247, pkaz}@jhu.edu)

²Dept. of Mechanical Engineering, Marmara University, Istanbul, 34722, Turkey (email: nural.yilmaz@marun.edu.tr, uqur.tumerdem@marmara.edu.tr)

by training in different configurations. In [27], a Gaussian process regression for end-to-end learning has been proposed to estimate the interaction forces on each jaw of the Raven II surgical system. However, the mentioned techniques cannot easily generalize to cases where the robot dynamics diverges from the initial training, for instance when instruments are changed during the operations.

To account for the uncertainty in the robot dynamics in a clinical setting, we proposed the use of neural networks [28] and transfer learning [29] for on the spot dynamic identification of the patient side manipulators of the da Vinci Research Kit (dVRK). However these works addressed force estimation in 3 and 6 axes (Cartesian translation and rotation), respectively, and like [19], [23], [24] neglected the gripper.

In this paper, we show that the gripping axis should not be neglected during training for dynamic identification and external force estimation, due to the inherently coupled structure of the da Vinci and its Endowrist instruments. We therefore propose an improved deep learning based dynamic identification method which also utilizes data from the gripper in training. With experiments and transfer learning we also demonstrate successful identification of the gripper as well as other joint dynamics with different instruments. The contributions of this paper can be summarized as:

- Extending the prior 6 DOF neural network for dynamic joint torque prediction to 7 DOF by adding gripper torque.
- Experimental verification that the accuracy of 6 DOF joint torque prediction is not significantly affected by gripper torque when the neural network training data includes gripper motion.
- Experimental verification that the grasping torque can be estimated by subtracting the free-space gripper torque predicted by the neural network from the measured gripper torque, and that transfer learning can quickly adapt this network to different instruments.
- Experimental evaluation of the accuracy of 7 DOF Cartesian force/torque estimation, including both the external 6 DOF wrench and 1 DOF grasping force.

The organization of the paper is as follows: Section II presents background information, including a description of the mechanical coupling in the dVRK, Section III introduces the deep learning based identification and external force estimation method, and Section IV provides the experimental results.

II. BACKGROUND

The generalized dynamic equation of the dVRK Patient Side Manipulator (PSM) can be described as:

$$M(q)\ddot{q} + C(q,\dot{q}) + G(q) + F(\dot{q}) + \tau_{int} + \tau_{ext} = \tau$$
 (1)

where q, \dot{q} and \ddot{q} denote the joint position, velocity and acceleration vectors. M is the mass/inertia matrix, C represents the Coriolis and centrifugal force/torque vector, and G is the gravity vector, while F represents the friction force/torque vector, τ_{int} represents the unmodeled internal robot dynamic



Fig. 1. Gripper Force-Torque Relationship

forces/torques and τ_{ext} represents any unmodeled external forces/torques.

The forces/torques on each joint due to external (contact) forces/torques are denoted with τ_{ext} , whereas τ denotes the joint actuation force/torque vector. From (1), external forces can be estimated:

$$\hat{\tau}_{ext} = \tau - \hat{\tau}_{dyn} \tag{2}$$

where $\hat{\tau}_{dyn} \approx M(q)\ddot{q} + C(q,\dot{q}) + G(q) + F(\dot{q}) + \tau_{int}$ represents the identified joint force/torques of the robot. Finally, the external forces acting on the end-effector in Cartesian space are computed using the Jacobian matrix (J) of the robot:

$$\hat{F}_{ext} = J^{-T} \hat{\tau}_{ext} \tag{3}$$

The above dynamics equation is expressed in the joint space of the robot and, in general, can include dynamic coupling between the joints because the mass/inertia matrix M typically has non-zero off-diagonal elements and the Coriolis/centrifugal and gravity vectors include coupling. Note that the Coriolis/centrifugal term is often written in matrix-vector form, $C(q,\dot{q})\dot{q}$, in which case C would be a matrix and could contain non-zero off-diagonal elements.

In addition to dynamic coupling, the PSM contains coupling in the transmission between the motors and joints of the instrument. In particular, the first-generation PSM contains 4 motors that drive wheels that engage with an attached surgical instrument (the most recent generation system has a similar structure, but with additional degrees of freedom for the instrument). There are multiple surgical instruments available to perform different tasks during the surgical procedure. The instruments typically define roll, pitch and yaw joints, as well as a grasper (or gripper), as shown in Figure 1. The mechanical design of the instrument introduces coupling between some of the drive wheels and some of the instrument joint motions. Thus, it is necessary to distinguish between actuator space (motors) and joint space (instrument). On the dVRK, the coupling between actuators and joints is one of the parameters specified in a Javascript Object Notation (JSON) file that describes a specific instrument. Figure 2 shows an example of the coupling matrix for the Cadiere Forceps. This coupling matrix converts actuator (motor) positions to joint positions and its transpose converts actuator torques to joint torques. The numeric values in the coupling matrix can vary between different instruments, but the general form is the same. For all currently supported instruments on the dVRK (except the three "snake-like" instruments), the only non-zero off-diagonal elements are as shown in Fig. 2.

Fig. 2. Actuator to joint position coupling matrix for Cadiere Forceps, P/N 400049. Joint order is roll, pitch, yaw, gripper.

The inverse of the matrix in Fig. 2 indicates that motion of the gripper joint requires coupled motion of the last two motors. However, the inverse of the transpose (converting joint torques τ_i to actuator torques τ_a) is the following:

$$\tau_a = \begin{bmatrix}
-0.6397 & 0.0 & 0.0 & 0.0 \\
0.0 & 0.9817 & 0.6696 & 0.6696 \\
0.0 & 0.0 & 0.8212 & 0.8212 \\
0.0 & 0.0 & -0.4106 & 0.4106
\end{bmatrix} \tau_j \tag{4}$$

This indicates that gripper torques are mechanically coupled with the last 3 motors. Thus, small errors in the coupling matrix could cause gripper torques to affect both the yaw and pitch joints.

We experimentally verified this hypothesis by moving the PSM through the same path (on joints 1-6), with three different configurations: (1) gripper at one of two fixed positions (0° and 40°) where no torque is applied, (2) gripper at -10°, where torque is applied on a piece of foam, and (3) gripper moving but not applying torque to an object. We generated the path by manually teleoperating the PSM with the Cadiere Forceps installed. We recorded the commanded position for each joint (except the gripper) and replayed the motion for other configurations of the gripper. While the manipulator is moving, joint position, velocity, and torque are measured. The maximum joint position of the pre-defined trajectory follows the maximal joint limit defined in the dVRK user manual.

The results are shown in Fig. 3 and demonstrate that gripper torques (including those due to motion) affect the measured pitch and yaw torques, presumably due to imperfections in the coupling matrix. The moving gripper also causes "noiser" torque measurements on joints 3 (insertion) and 4 (roll), which could be due to dynamic coupling effects from Eq. 1 or to other factors such as vibrations caused by the gripper motion.

These results suggest that gripper states must be included as input while generating PSM body networks for J3-J6 to identify robot inverse dynamics because PSM joint dynamic forces/torques change with gripper motion in these axes due to the mechanical coupling and/or vibration.

III. LEARNING BASED DYNAMIC DECOUPLING AND DYNAMIC IDENTIFICATION

The proposed method is to model the inverse dynamics of a dVRK PSM by eliminating coupling between the wrist and the gripper based on a learning approach.

In our previous work [28], [29], we proposed a neural network-based dynamic identification method to estimate

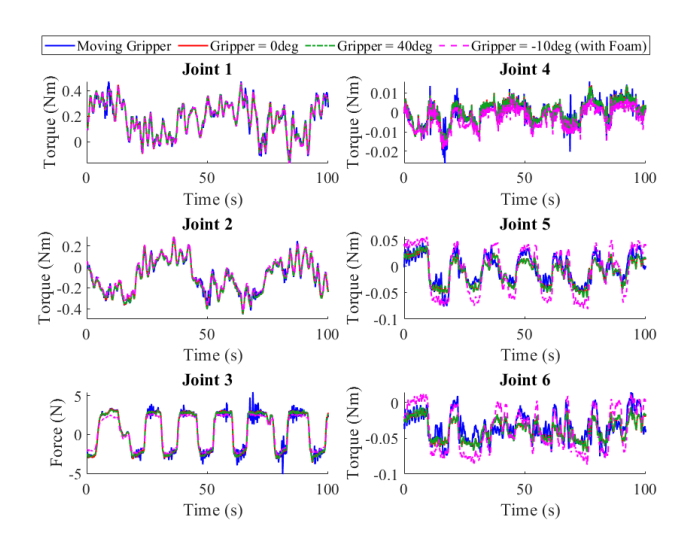


Fig. 3. Measured joint torques using the same excitation path for 4 cases: Gripper moving, constant at 0° , 40° and -10° holding a thin piece of foam.

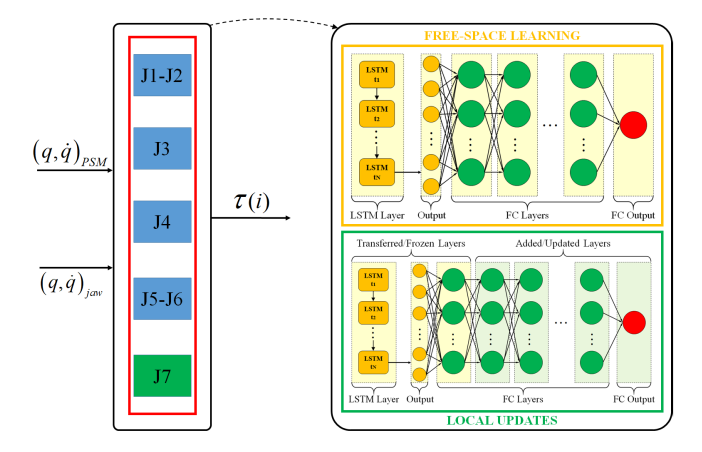


Fig. 4. Network Structure. Blue rectangles: PSM body joints, Green rectangle: Gripper

joint force/torques excluding the gripper axis, which was not moving or grasping objects in those experiments. However, as discussed in Section II, the coupled structure of the dVRK Endowrist instruments must be considered. Although the use of a coupling matrix is intended to resolve the problem, Section II demonstrated that coupling between the gripper and other joints remains an issue. In this paper, we extend our previous work by proposing an improved deep learning-based method making use of gripper states in addition to the other PSM joint states provided by the dVRK. Furthermore, during operation, instrument changes are frequently necessary, and therefore we propose a transfer learning-based identification method that can quickly adapt the main network to the new instrument (in addition to other patient/setup specific factors).

The identification method makes use of free space networks (**FS**) trained with extensive data covering the robot's workspace. The purpose of this is to teach the robot the general behavior of the robot dynamics. Since this training is outside the patient, training and computation power do not have any impact on the surgery. The initial experimental results shown in Fig. 3 and discussed in Section II suggest that the network for the last 4 joints must include the gripper

Train	Test	J1	J2	J3	J4	J5	J6
C	C	5.29(0.94)	5.73(0.60)	7.72(0.90)	3.50(0.44)	3.69(0.46)	3.69(0.64)
M	M	6.50(0.92)	6.98(0.66)	5.72(0.70)	1.99(0.19)	3.34(0.57)	3.64(0.60)
С				7.51(0.91)			
M	C	6.14(0.49)	7.73(1.08)	10.24(3.57)	3.99(0.68)	5.06(0.59)	7.71(0.89)
				6.11(0.94)			
M+C	C	6.04(0.82)	5.88(0.67)	7.20(1.72)	3.67(0.45)	3.74(0.60)	3.81(0.54)

TABLE I

NRMSE RESULTS OF COUPLING EXPERIMENTS (%). M: GRIPPER IS MOVING, C: GRIPPER IS CLOSED

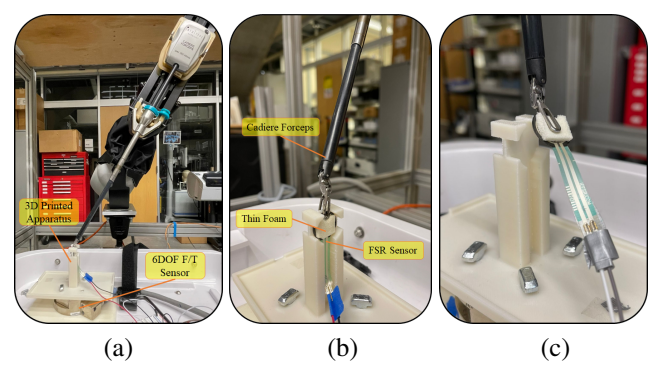


Fig. 5. 7 DOF experimental setup: (a) Grasping the FSR mounted on the apparatus attached to the ATI force sensor, (b) closeup view, (c) FSR held by gripper while instrument pushes against side of apparatus.

axis, as shown in Fig. 4.

IV. EXPERIMENTAL SETUP AND RESULTS

This section presents the experiments. First, we evaluate the accuracy of dynamic torque estimation of the robot joints (not including the gripper) when the gripper is moving, to show that higher accuracy is obtained when the neural network training data includes a moving gripper. Next, we add a neural network for dynamic gripper torque estimation and show that transfer learning can adapt this network to different instruments. Then, we show that subtracting the predicted dynamic gripper torque from the measured gripper torque can provide a reasonable estimate of grasping force. Finally, we show that the proposed system can simultaneously estimate the 6 DOF external wrench and 1 DOF grasp force.

For the data used in the free space training of the networks, we generate excitation paths for the manipulators in the joint space in order to move the robot at different velocities. A random number generator with a nonrepeatable uniform output created the raw path, which is smoothed by two low pass filters to make the trajectory achievable on the dVRK. The maximum and minimum values of the generator are based on the specified joint limits of the dVRK so that the path covers the entire workspace of the robot. In total, around 15 minutes of data (joint positions, joint velocities, and joint torques) were collected and split into training, validation, and test sets using a 5:1:1 ratio.

For some experiments, we used an ATI Gamma force/torque sensor (ATI Industrial Automation, Apex, NC, USA), attached to a fixed apparatus, to provide ground truth 6 DOF measurements. In addition, we used a force-sensing resistor (FSR) to measure grip forces. Figure 5 depicts the experimental

setups used for Sections IV-C and IV-D. The FSR sensor feedback is calibrated using the ATI sensor. We attached the FSR directly on the ATI and press the FSR to get readings from both sensors. We fit a polynomial, as shown in eq. (5), where x is the raw FSR voltage reading (range 0-1 V) and F is the force in Newtons, to calibrate the FSR with respect to the ATI force.

$$F = 3.71x^3 - 4.63x^2 + 2.57x + 0.105V \tag{5}$$

A. Dynamic Torque Estimation with Moving Gripper

The goal of this experiment is to determine whether it is necessary to include gripper motion in the training data used to estimate the dynamic torque for the robot joints, especially for joints 3-6. We trained one set of neural networks using the excitation path described above, without moving the gripper or applying a grip torque (C). We then trained another set of neural networks using the same excitation path, but including gripper motion (M). Finally, we trained a third set of neural networks using 3 datasets with a moving gripper and 2 datasets with a closed gripper (C+M).

Table I shows the results of testing each of these networks with trajectories that included (M) or did not include (C) gripper motion. As expected, networks trained with only one condition (C or M) performed well when tested under that same condition, but poorly when tested under the opposite condition, especially for J5 and J6 where the gripper torques are mechanically coupled to those joints. However, some decrease in performance is also seen in other joints. In contrast, training the neural network with both conditions (C+M) provides good performance when tested under either condition. Some sample plots are shown in Fig. 6.

B. Transfer Learning for Gripper Dynamics Identification

The goals of this experiment are to demonstrate that the neural network can be trained to estimate the dynamics torque of an instrument gripper but, more importantly, that transfer learning can be used to quickly adapt this network to different instruments. The experiment was performed extracorporeally with 8 different instruments: Large Needle Driver (LND), Small Clip Appliers (SCA), Resano Forceps (RF), Monopolar Curved Scissors (MCS), Maryland Bipolar Forceps (MBF), Prograps Forceps (PF), Cadiere Forceps (CF), and Long Tip Forceps (LTF), which are shown in Figure 7. Since each instrument has different geometry, jaw limits and coupling system, they have different dynamics properties. Therefore, it is important to update the network quickly to adapt it to a new dynamics in case of instrument changes during surgery.

The **FS** network was generated using a Large Needle Driver (LND) and tested on all instruments. To eliminate the errors caused by the differences due to the instrument changes, individual transfer learning networks **Xfer** were trained using the corresponding instruments. To train these networks, 3 min training, 1 min evaluation and 1 min test sets were collected and replayed for all of the instruments. To collect data, the robot was moved to different poses with different velocities in its workspace and the gripper was opened and closed during

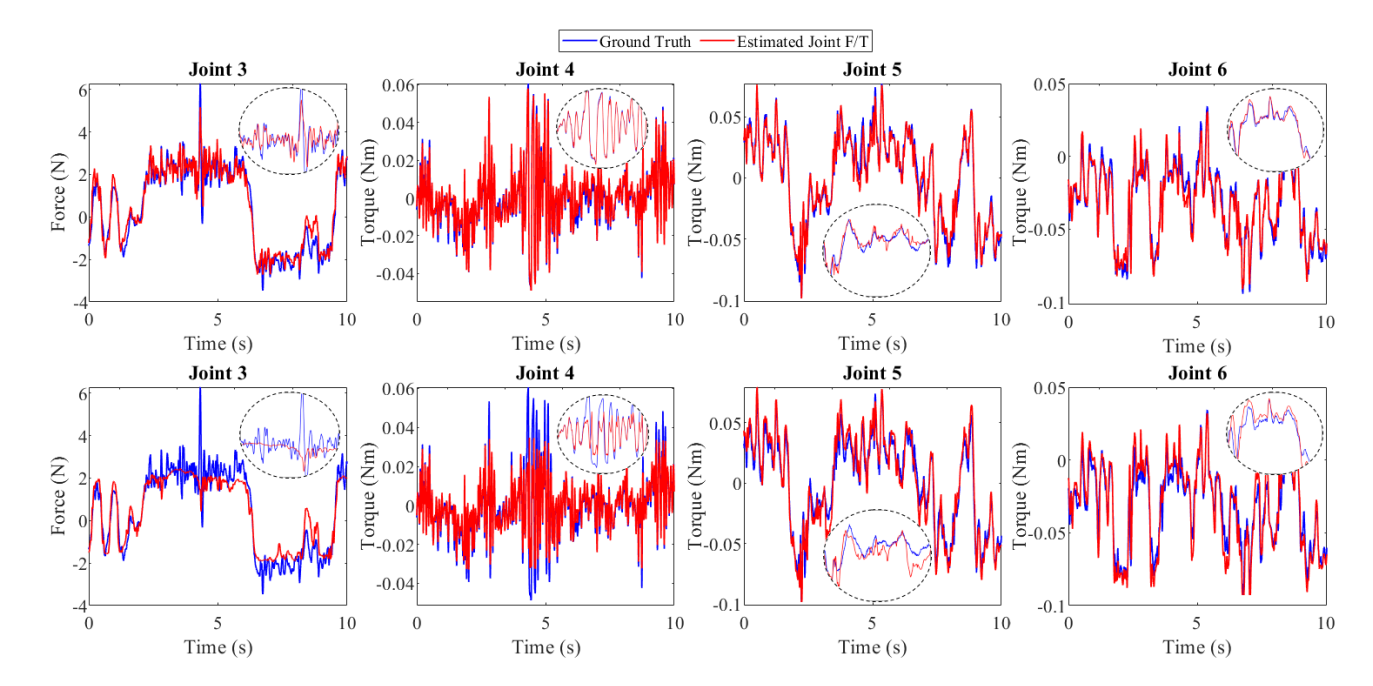


Fig. 6. Test results with trajectories that include a moving gripper. **Top:** Network trained with moving gripper. **Bottom:** Network trained with closed gripper. As expected, network trained with closed gripper does not perform as well when tested with moving gripper.



Fig. 7. Different instruments utilized in the experiments: (a) Large Needle Driver, (b) Cadiere Forceps, (c) Long Tip Forceps, (d) Monopolar Curved Scissors, (e) Maryland Bipolar Forceps, (f) Prograsp Forceps, (g) Resano Forceps, (h) Small Clip Appliers.

the motion. Table II shows the Normalized Root Mean Square Error (NRMSE) of the test results and it can be seen that there is a significant error in identification in case of the **FS** network for each instrument after remounting them, but **Xfer** provides considerable improvement where NRMSE values vary from 5% to 8% in the gripper axis. Therefore, it can inferred that **Xfer** is able to adapt the network to the instrument changes.

C. Gripper Force Estimation

We performed two experiments, using the Cadiere Forceps, to evaluate the gripper force estimation, using the FSR as a ground truth. The external gripper torque is estimated by subtracting the free-space torque predicted by the neural

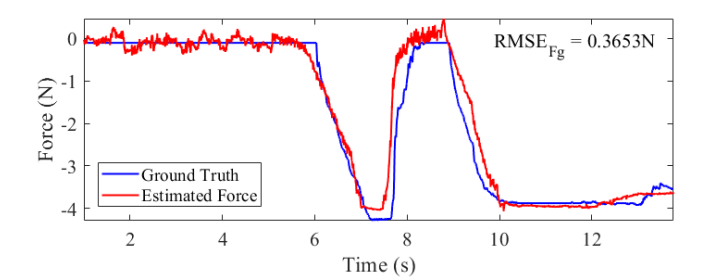


Fig. 8. Comparison of the FSR force and estimated gripper force

network from the measured joint torque. Note, however, that we estimate a gripper torque whereas the FSR measures a gripper force. In principle, gripper force and torque can be related if the distance between the torque axis (gripper pivot) and the force contact point (i.e., d_{force} in Fig. 1) is precisely known. In practice, however, it can be difficult to accurately measure d_{force} , especially since it may not be valid to model the contact between the jaw and the FSR as a point contact. Therefore, we empirically determined the scale factor between gripper forces and torques.

In the first experiment, we show the dynamic performance of the gripper torque estimation by grasping and releasing the FSR, which is attached to the fixed apparatus, at a fixed pose

TABLE II

MEAN (STD. DEV.) OF NRMSE OF ESTIMATED GRIPPER TORQUE FOR DIFFERENT INSTRUMENTS, WHEN ESTIMATED BY A NETWORK TRAINED WITH A LARGE DATASET COLLECTED WITH THE LND INSTRUMENT (FS) AND A NETWORK TRAINED VIA TRANSFER LEARNING WITH A SMALL SAMPLE OF DATA FROM THAT INSTRUMENT (XFER).

	CF	LTF	MCS	MBF	PF	RF	SCA
FS (%)	26.662 (2.184)	29.942 (2.951)	29.087 (7.678)	30.919 (2.353)	20.750 (1.953)	26.734 (2.267)	38.384 (4.982)
Xfer (%)	6.033 (1.350)	7.722 (1.828)	5.039 (0.730)	7.768 (2.131)	4.985 (0.589)	6.878 (1.048)	5.391 (1.016)

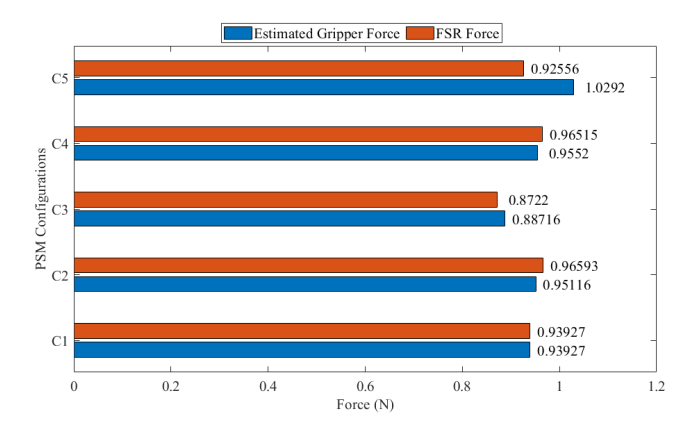


Fig. 9. Estimated gripper force compared to ground truth (FSR). J5 and J6 joint angles for each configuration (C): C1: $[0^o, 0^o]$, C2: $[60^o, 0^o]$, C3: $[30^o, 0^o]$, C4: $[0^o, 60^o]$, C5: $[0^o, 30^o]$. Estimated gripper torque converted to force using empirical scale factor computed at C1.

of the gripper, as shown in Fig. 5(a),(b). The result of this experiment is shown in Fig. 8, with an empirically determined scale factor of $50\,m^{-1}$ to convert the predicted torque (Nm) to the predicted force (N). As shown in this figure, the gripper force estimated by the network is in agreement with the ground truth forces provided by the FSR. The normalized RMS error (NRMSE, as defined in [24] and [28]) of gripper force estimation is 8.73%, and the RMSE error is 0.37 N for roughly 13 seconds of operation.

In the second experiment, we move the manipulator to 5 different configurations with the gripper holding the FSR at a fixed angle. For these configurations, joints 1, 2 and 4 are fixed at 0 degrees and joint 3 at 135 mm, while joints 5 and 6 are varied. In this experiment, we hold the gripper at a fixed angle and therefore expect that the force value should not change as joints 5 and 6 are moved. We empirically determine the scale factor between the estimated gripper torque and measured FSR force at configuration 1 (J5 and J6 at 0 degrees) and use this value for the other configurations. The result is shown in Fig. 9. In the figure, it is evident that the force measured by the FSR changes as the wrist is moved, even though the desired gripper angle remained constant. Some of this variation is due to the measured joint angle varying between -9.70 and -9.84 degrees, presumably due to control system error. Other potential factors include inaccuracy of the FSR, changes in gravity and/or drag caused by the electrical wires attached to the FSR, and uncompensated coupling between the gripper and the other wrist joints. In other words, even if the controller can maintain the gripper joint angle at a constant value based on the measured joint angle, the actual joint angle may vary due to coupling. Nevertheless, the figure also shows that, in most cases, the estimated gripper force closely follows the variation in the measured gripper force.

D. Estimation of 7 DOF External Forces/Torques

This experiment evaluates the performance of the neural network for estimating both 6 DOF external force/torque and 1 DOF gripper force. We moved the gripper to touch the apparatus from multiple different directions several times while holding the FSR at roughly the same angle during the

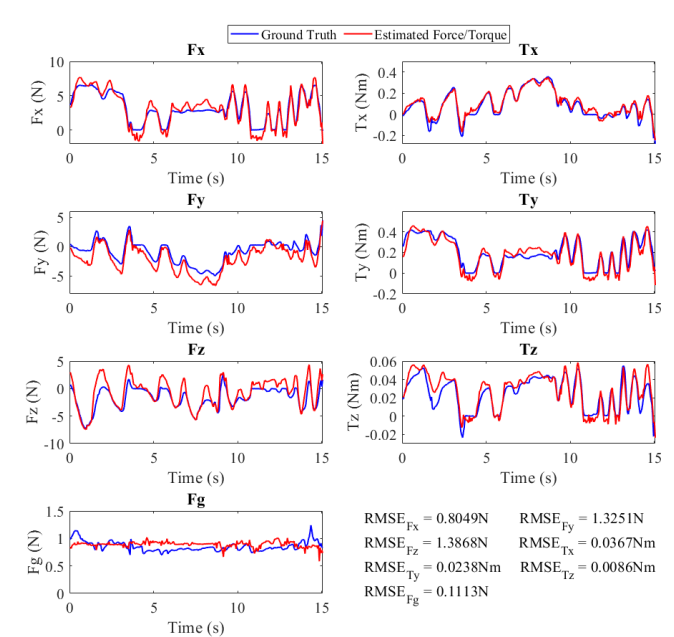


Fig. 10. 7 DOF force/torque estimation results

experiment, as shown in Fig. 5(c). The apparatus was attached to an ATI force sensor that provided 6 DOF ground-truth force/torque measurement and the FSR provided 1D ground-truth gripper force measurement. As shown in Fig. 10, the RMSE for Cartesian space forces are less than 1.4 N whereas the RMSE for Cartesian space torques are less than 0.06 Nm in each axis. This represents a small loss of accuracy compared to our prior work [29], which did not include estimation of grasping force.

V. CONCLUSION

In this work, we demonstrate that neural networks can predict the dynamics torques of the gripper in addition to the other 6 joints of the dVRK PSM, even though there is mechanical coupling between the gripper and some of the wrist joints. This enables simultaneous estimation of the 6 DOF force/torque applied on the environment and the 1 DOF grasp force. We also demonstrate that our selfsupervised transfer learning approach [29] can quickly adapt the neural network to other instruments. External forces and torques are estimated with RMS errors of 1.4 N and 0.04 Nm, respectively, which represents a small decrease in accuracy, due to the inclusion of an active gripper, with respect to our prior work with a fixed gripper. Grasping forces were estimated with an accuracy of approximately 0.1 N, after empirically determining the scale factor between gripper torque and applied force.

VI. ACKNOWLEDGEMENTS

This work was supported in part by NSF OISE 1927354. We thank Jie Ying Wu for assisting with the experimental setup.

REFERENCES

- [1] U. Hagn, R. Konietschke, A. Tobergte, M. Nickl, S. Jörg, B. Kübler, G. Passig, M. Gröger, F. Fröhlich, U. Seibold, L. Le-Tien, A. Albu-Schäffer, A. Nothhelfer, F. Hacker, M. Grebenstein, and G. Hirzinger, "DLR MiroSurge: a versatile system for research in endoscopic telesurgery," *International Journal of Computer Assisted Radiology and Surgery*, vol. 5, no. 2, pp. 183–193, Mar 2010.
- [2] B. Hannaford, J. Rosen, D. Friedman, H. King, P. Roan, L. Cheng, D. Glozman, J. Ma, S. N. Kosari, and L. White, "Raven-II: An open platform for surgical robotics research," *IEEE Trans. on Biomedical Engin.*, vol. 60, no. 4, pp. 954–959, Apr 2013.
- [3] P. J. Berkelman, L. L. Whitcomb, R. H. Taylor, and P. Jensen, "A miniature microsurgical instrument tip force sensor for enhanced force feedback during robot-assisted manipulation," *IEEE Transactions on Robotics and Automation*, vol. 19, no. 5, pp. 917–921, 2003.
- [4] U. Seibold, B. Kubler, and G. Hirzinger, "Prototype of instrument for minimally invasive surgery with 6-axis force sensing capability," in *IEEE Intl. Conf. on Robotics and Automation*. IEEE, 2005, pp. 496–501.
- [5] U. Kim, D.-H. Lee, W. J. Yoon, B. Hannaford, and H. R. Choi, "Force sensor integrated surgical forceps for minimally invasive robotic surgery," *IEEE Transactions on Robotics*, vol. 31, no. 5, pp. 1214–1224, 2015.
- [6] R. Pena, M. J. Smith, N. P. Ontiveros, F. L. Hammond, and R. J. Wood, "Printing strain gauges on Intuitive Surgical da Vinci robot end effectors," in *Intl. Conf. on Intelligent Robots and Systems*. IEEE, Oct 2018, pp. 806–812.
- [7] J. Peirs, J. Clijnen, D. Reynaerts, H. Van Brussel, P. Herijgers, B. Corteville, and S. Boone, "A micro optical force sensor for force feedback during minimally invasive robotic surgery," *Sensors and Actuators A: Physical*, vol. 115, no. 2-3, pp. 447–455, 2004.
- [8] K. Tadano and K. Kawashima, "Development of 4-DOFs forceps with force sensing using pneumatic servo system," in *Intl. Conf. on Robotics* and Auto. IEEE, 2014, pp. 2250–2255.
- [9] N. Yilmaz, M. Bazman, and U. Tumerdem, "External force/torque estimation on a dexterous parallel robotic surgical instrument wrist," in *IEEE/RSJ Intl. Conf. on Intelligent Robots and Systems (IROS)*. IEEE, 2018, pp. 4396–4403.
- [10] M. Jinno, "Simple noninterference mechanism between the pitch and yaw axes for a wrist mechanism to be employed in robot-assisted laparoscopic surgery," *ROBOMECH Journal*, vol. 6, no. 1, pp. 1–12, 2019.
- [11] L. Yu, Y. Yan, X. Yu, and Y. Xia, "Design and realization of forceps with 3-d force sensing capability for robot-assisted surgical system," *IEEE Sensors Journal*, vol. 18, no. 21, pp. 8924–8932, 2018.
- [12] L. N. Verner and A. M. Okamura, "Effects of translational and gripping force feedback are decoupled in a 4-degree-of-freedom telemanipulator," in Second Joint EuroHaptics Conference and Symposium on Haptic Interfaces for Virtual Environment and Teleoperator Systems (WHC'07). IEEE, 2007, pp. 286–291.
- [13] Y. Liang, Z. Du, W. Wang, Z. Yan, and L. Sun, "An improved scheme for eliminating the coupled motion of surgical instruments used in laparoscopic surgical robots," *Robotics and Autonomous Systems*, vol. 112, pp. 49–59, 2019.
- [14] W. Hong, A. Schmitz, W. Bai, P. Berthet-Rayne, L. Xie, and G.-Z. Yang, "Design and compensation control of a flexible instrument for endoscopic surgery," in *IEEE International Conference on Robotics and Automation (ICRA)*. IEEE, 2020, pp. 1860–1866.
- [15] L. Yu, X. Yu, and Y. Zhang, "Microinstrument contact force sensing based on cable tension using BLSTM-MLP network," *Intelligent Service Robotics*, vol. 13, no. 1, pp. 123–135, 2020.
- [16] P. Kazanzides, Z. Chen, A. Deguet, G. S. Fischer, R. H. Taylor, and S. P. DiMaio, "An open-source research kit for the da Vinci® surgical system," in *IEEE Intl. Conf. on Robotics and Auto. (ICRA)*, Hong Kong, China, Jun 2014, pp. 6434–6439.
- [17] C. D'Ettorre, A. Mariani, A. Stilli, F. Rodriguez y Baena, P. Valdastri, A. Deguet, P. Kazanzides, R. H. Taylor, G. S. Fischer, S. P. DiMaio, A. Menciassi, and D. Stoyanov, "Accelerating surgical robotics research: A review of 10 years with the da Vinci Research Kit," *IEEE Robotics and Automation Magazine*, vol. 28, no. 4, pp. 56–78, Dec. 2021.
- [18] B. Hannaford, J. Rosen, D. W. Friedman, H. King, P. Roan, L. Cheng, D. Glozman, J. Ma, S. N. Kosari, and L. White, "Raven-II: an open platform for surgical robotics research," *IEEE Trans. on Biomedical Engineering*, vol. 60, no. 4, pp. 954–959, 2012.

- [19] N. Tran, J. Y. Wu, A. Deguet, and P. Kazanzides, "A deep learning approach to intrinsic force sensing on the da Vinci surgical robot," in *IEEE Intl. Conf. on Robotic Computing*, Nov. 2020, pp. 25–32.
- [20] G. A. Fontanelli, L. R. Buonocore, F. Ficuciello, L. Villani, and B. Siciliano, "A novel force sensing integrated into the trocar for minimally invasive robotic surgery," in *IEEE/RSJ Intl. Conf. on Intelligent Robots and Systems (IROS)*. IEEE, 2017, pp. 131–136.
- [21] Y. Wang, R. Gondokaryono, A. Munawar, and G. S. Fischer, "A convex optimization-based dynamic model identification package for the da Vinci Research Kit," *Robotics and Automation Letters*, pp. 3657–3664, 2019
- [22] M. Haghighipanah, M. Miyasaka, and B. Hannaford, "Utilizing elasticity of cable-driven surgical robot to estimate cable tension and external force," *IEEE Robotics and Automation Letters*, vol. 2, no. 3, pp. 1593–1600, 2017.
- [23] H. Sang, J. Yun, R. Monfaredi, E. Wilson, H. Fooladi, and K. Cleary, "External force estimation and implementation in robotically assisted minimally invasive surgery," *The International Journal of Medical Robotics and Computer Assisted Surgery*, vol. 13, no. 2, p. e1824, 2017.
- [24] F. Piqué, M. N. Boushaki, M. Brancadoro, E. De Momi, and A. Menciassi, "Dynamic modeling of the da Vinci research kit arm for the estimation of interaction wrench," in *International Symposium* on *Medical Robotics (ISMR)*. IEEE, 2019, pp. 1–7.
- [25] J. J. O'Neill, T. K. Stephens, and T. M. Kowalewski, "Evaluation of torque measurement surrogates as applied to grip torque and jaw angle estimation of robotic surgical tools," *Robotics and Automation Letters*, vol. 3, no. 4, p. 3027, 2018.
- [26] Y. Guo, B. Pan, Y. Fu, and M. Q.-H. Meng, "Grip force perception based on dAENN for minimally invasive surgery robot," in *IEEE Intl. Conf. on Robotics and Biomimetics (ROBIO)*. IEEE, 2019, pp. 1216–1221.
- [27] Y. Li and B. Hannaford, "Gaussian process regression for sensorless grip force estimation of cable-driven elongated surgical instruments," *IEEE Robotics and Automation Letters*, vol. 2, no. 3, pp. 1312–1319, 2017.
- [28] N. Yilmaz, J. Y. Wu, P. Kazanzides, and U. Tumerdem, "Neural network based inverse dynamics identification and external force estimation on the da Vinci Research Kit," in *IEEE Intl. Conf. on Robotics and Automation (ICRA)*. IEEE, 2020, pp. 1387–1393.
- [29] N. Yilmaz, J. Zhang, P. Kazanzides, and U. Tumerdem, "Transfer of learned dynamics between different surgical robots and operative configurations," in *International Conference on Information Processing* in Computer-Assisted Interventions (IPCAI), 2022.